Materials Science and Engineering A 528 (2011) 1138–1142

Contents lists available at ScienceDirect

Materials Science and Engineering A

journal homepage: www.elsevier.com/locate/msea

A comparative study of laser beam welding and laser–MIG hybrid welding of Ti–Al–Zr–Fe titanium alloy

Ruifeng Li[a,b], Zhuguo Li[a,*], Yanyan Zhu[a], Lei Rong[a]

[a] Shanghai Key Laboratory of Materials Laser Processing and Modification, Shanghai Jiao Tong University, Shanghai 200240, People's Republic of China
[b] School of Materials Science and Engineering, Jiangsu University of Science and Technology, Zhenjiang Jiangsu 212003, People's Republic of China

ARTICLE INFO

Article history:
Received 24 May 2010
Received in revised form
26 September 2010
Accepted 27 September 2010

Keywords:
Ti–Al–Zr–Fe titanium alloy
Laser beam welding
Laser–MIG hybrid welding
Joint properties

ABSTRACT

Ti–Al–Zr–Fe titanium alloy sheets with thickness of 4 mm were welded using laser beam welding (LBW) and laser-MIG hybrid welding (LAMIG) methods. To investigate the influence of the methods difference on the joint properties, optical microscope observation, microhardness measurement and mechanical tests were conducted. Experimental results show that the sheets can be welded at a high speed of 1.8 m/min and power of 8 kW, with no defects such as, surface oxidation, porosity, cracks and lack of penetration in the welding seam. In addition, all tensile test specimens fractured at the parent metal. Compared with the LBW, the LAMIG welding method can produce joints with higher ductility, due to the improvement of seam formation and lower microhardness by employing a low strength TA-10 welding wire. It can be concluded that LAMIG is much more feasible for welding the Ti–Al–Zr–Fe titanium alloy sheets.

1. Introduction

With the properties of low density, excellent high temperature mechanical properties and good corrosion resistance, titanium and titanium alloys have widely and successfully used in the medical, aerospace, automotive, petrochemical, nuclear and power generation industries [1,2]. Ti–Al–Zr–Fe is a medium strength, near-α type titanium alloy. This near-α titanium alloy was developed to meet the need for the cold working structures. As an alloy element, Fe could reduce the cost and accelerate the application of this alloy [3]. With the development of titanium industries, many welding methods such as gas tungsten arc welding [4,5], electron beam welding [5–7], friction welding [8] and laser welding [9–12] have already been developed.

Because of their high chemical activity, titanium alloys are easy to absorb harmful gas. As a result, reliability problems such as low mechanical properties and unstable structure would be induced. Nonetheless, laser welding has considerable flexibility for joining titanium alloys. As laser welding permits the generation of a keyhole that effectively concentrates the energy input into a small area, there is a good potential to join titanium alloys, meanwhile, the microstructural changes are confined to the fusion region and narrow heat affected zone, which has been reported to conserve the corrosion resistance and mechanical strength of the welding joints [9–12]. However, disadvantages of the wider use of the laser welding process are the insufficient gap bridging ability and the required precision in positioning. The combination of laser welding with either TIG/GTAW or MIG/GMAW is referred to as hybrid welding. The hybrid laser welding has proven to resolve these drawbacks of laser welding, while maintaining the key advantages of laser welding and even improving the welding speed and penetration [13–16].

This investigation aimed at contributing to an improved understanding of the influence of the LBW and LAMIG welding methods on the properties of Ti–Al–Zr–Fe titanium alloy joints. The influence of methods difference on welding bead appearance, interfacial microstructure and mechanical properties were analyzed systematically.

2. Experimental materials and methods

The welding experiments were carried out on the Ti–Al–Zr–Fe alloy sheets with a dimension of 200 mm × 100 mm × 4 mm. The chemical compositions of Ti–Al–Zr–Fe are shown in Table 1. In the LAMIG process, TA-10 filler wire with 1.2 mm diameter was used. The chemical compositions of TA-10 are shown in Table 1.

A 15 kW continuous CO_2 laser (TRUMPF TLF15000) was used to weld the titanium sheets. The experimental setup of the LAMIG process is shown in Fig. 1. For LBW process, there is no MIG torch

* Corresponding author at: Shanghai Key Laboratory of Materials Laser Processing and Modification, Shanghai Jiao Tong University, No. 800, Dongchuan Road, Shanghai, 200240, People's Republic of China. Tel.: +86 21 54748940; fax: +86 21 34202814.
E-mail address: lizg@sjtu.edu.cn (Z. Li).

0921-5093/$ – see front matter © 2010 Elsevier B.V. All rights reserved.
doi:10.1016/j.msea.2010.09.084

Table 1
Chemical compositions of Ti–Al–Zr–Fe titanium alloy [3] and TA-10 welding wire (wt.%).

	Al	Mo	Zr	Fe	Ni	Si	C	N	H	O	Ti
Ti–Al–Zr–Fe	2.0–3.0	–	2.0	1.0–1.1	–	<0.02	0.01	0.02	0.001	0.07–0.09	Balance
TA-10	–	0.2~0.4	–	≤0.30	0.6~0.9	–	≤0.08	≤0.30	≤0.015	≤0.25	Balance

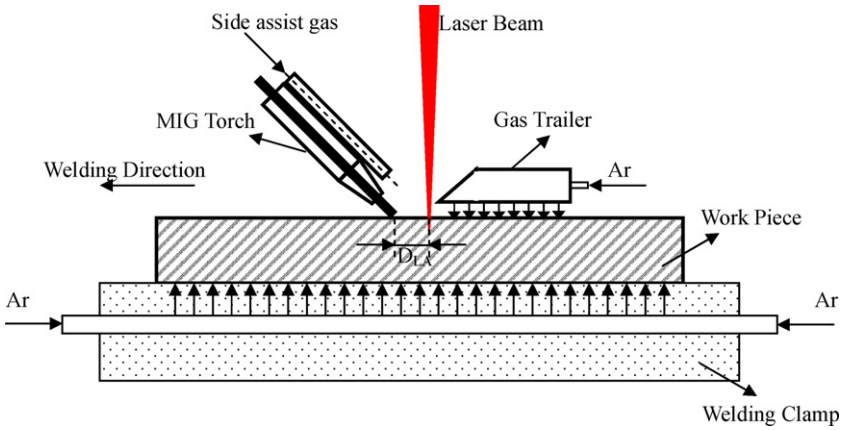

Fig. 1. Experimental setup of LAMIG welding process.

Table 2
Welding parameters.

Welding Method	Parameters								
	Power (kW)	Welding speed (m/min)	Wire feed speed (m/min)	Arc voltage (V)	Laser-arc distance (D_{LA}, mm)	Clearance (mm)	MIG gas flow rate (L/min)	Side assist gas flow rate (L/min)	Focal position (mm)
LBW	8	1.8	–	–	–	–	–	30	−2
LAMIG	8	1.8	10	30	6	0.5	25	30	−2

used. A copper backing plate with clamps was used for formation of the weld root with narrow bead of weld and low angle distortions of joints. During the welding process, the laser beam was focused on 2 mm with a radius of 0.8 mm under the surface of the sheets to obtain enough penetration. A trailing and back shielding gas supplied by ultra high purity argon gas were both at flow rates of 25 L/min to protect the melt pool and heat affected zone (HAZ) from oxidation. Side assist gas of He was used both to protect the welding pool and to decrease the laser plasma formed during the welding process. The welding parameters are shown in Table 2.

After welding, digital photographs were used to capture the bead appearance. Then the specimens were sectioned transverse to the welding direction, polished and etched. Optical microscope and Vickers hardness tester (HVS-10) were used to obtain the interfacial microstructure and microhardness of the seam. In addition, the standard tensile and bending samples were prepared. Tensile testing was performed at room temperature using a Zwick Roell tensile test machine.

3. Experimental results and discussions

3.1. Appearance of weld

Fig. 2 shows the front and back bead surface appearance of the joints welded with LBW and LAMIG methods. It can be seen that both bead formation are regular and uniform in a bright sliver color. No defects like oxidation or lack of penetration were found in the welding joints. It was also found that the 4 mm Ti–Al–Zr–Fe titanium alloy sheets can be welded at a high speed of 1.8 m/min (3–4 times bigger than that of TIG welding process) as the laser power is 8 kW.

Fig. 2 shows the cross section profile of the LBW and LAMIG welds. Satisfactory joints are achieved, regarding both to the full penetration and low distortion. The bead profile is regular and uniform, without cracks and porosities in the seam. Fig. 3a also indicates there is a light undercut in the LBW weld. The reason for undercut may be the overlarge welding speed during the LBW

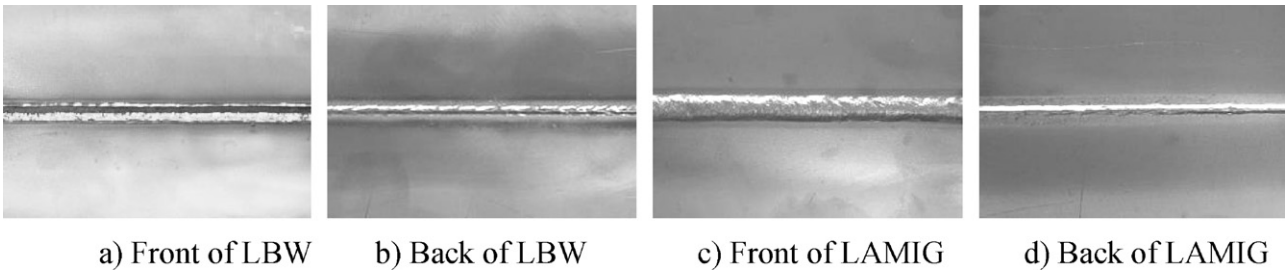

Fig. 2. Front and back bead appearance of Ti–Al–Zr–Fe LBW and LAMIG welded joints.

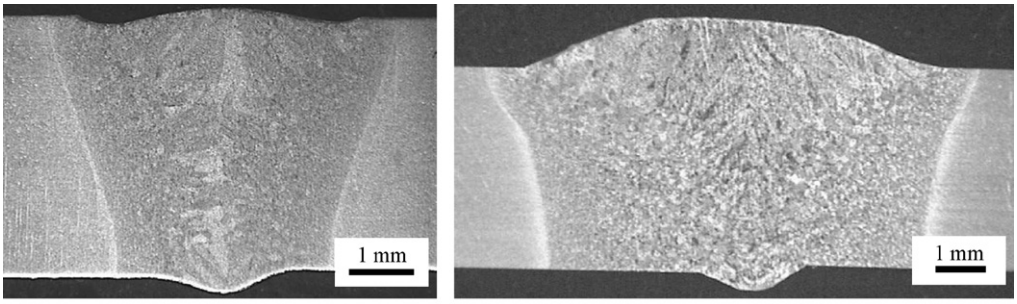

Fig. 3. Cross-section profile of LBW and LAMIG welded joints.

welding process. At low welding speed, the melted metal can have enough time to flow and spread to the edge of welding seam due to the "keyhole" action of LBW. But at overlarge welding speed, the melted welding pool solidified quickly leading to less time and liquid metal to fill the edge of the welding seam [17,18]. Nevertheless, Fig. 3b shows a slightly protruding top surface and smooth transition from the weld metal to the parent metal in the LAMIG welded joint with the same high welding speed as in LBW. For LAMIG process, the cooling speed is much lower due to higher heat input; in addition the melted welding wire can introduce much more liquid metal to the welding seam than LBW process, so there are no undercut defects found in LAMIG process. Because the arc has a relatively broad heating area, the width of the LAMIG weld seam is much bigger than that of the LBW weld seam. Even at a relatively low magnification, evidence of coarse, columnar prior-β grains which nucleated epitaxiaily from the base metal substrate and grew toward the weld centreline can be observed from Fig. 3.

3.2. Interfacial microstructure

Examination of the laser weld fusion zone, HAZ and parent metal (PM) zone at increased magnification using an optical microscope are shown in Fig. 4. Fig. 4a reveals a fine acicular α′ solidification structure within the prior-β column grains in the fusion zone after LBW process. The prior-β grain of fusion zone in LAMIG welded joint is much bigger than that in LBW welded joint due to the large heat input of MIG arc. The microstructures of HAZ and PM in LBW and LAMIG joint are much similar. Both the HAZ consist of martensitic α′, acicular α and primary β.

3.3. Mechanical properties

Fig. 5 shows the microhardness distribution on the cross-section of the LBW and LAMIG welded joints. In the LBW welded joints, the microhardness increased a lot from 250 HV to 300 HV or so, as shown in Fig. 4a. The observed large increase of microhardness in

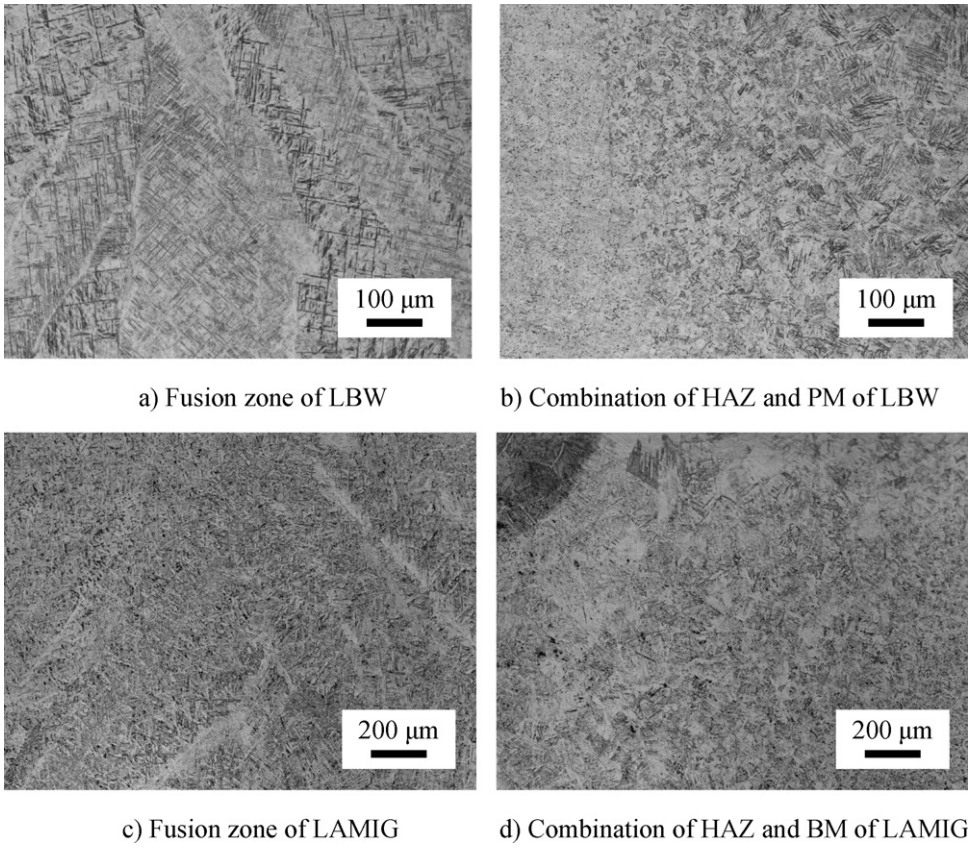

Fig. 4. Interfacial microstructure of LBW and LAMIG welded joints.

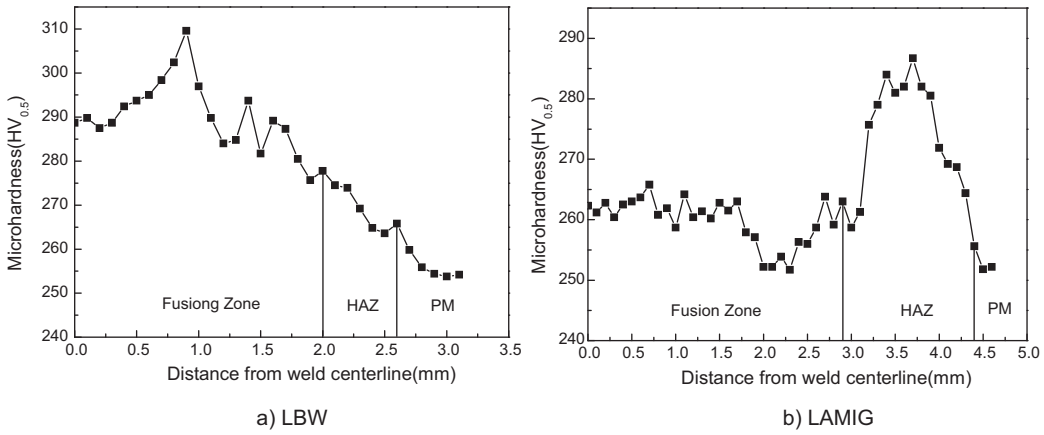

Fig. 5. Microhardness distribution on the cross-section of LBW and LAMIG welded joints.

Table 3
Tensile and bending test results of parent metal, LBW and LAMIG welded joints.

Welding process	Tensile test		Bending test	
	σ_b(MPa)	Fracture location	Face bending angle (°)	Root bending angle (°)
Parent metal	690	–	>120	–
LBW	696	Parent metal	90 (fusion line)	>120
LAMIG	709	Parent metal	>120	>120

the Ti–Al–Zr–Fe welded joint is due to a high cooling rate associated with LBW process. In the LAMIG welded joints, the microhardness in the fusion zone is much lower than that in the LBW joints. The reasons may be the less cooling speed and the low strength-index TA-10 wire used in the LAMIG process.

Table 3 shows the tensile and bending test results of the LBW, LAMIG welded joints and the parent metal. The fracture of both LBW and LAMIG welding joints occurred at the parent metals as shown in Fig. 6. The tensile strength (σ_b) is higher than that of the parent metals'. The bending test results are a good evidence of plasticity index. It can be seen that the LBW welded joint fractured at the fusion line when the face bending angle is 90°. Possible reasons are the high stress concentration at the undercut location on the LBW seam surface and the low ductility due to the formation of high cross-section microhardness structure. As shown in Table 3, no fracture happened when the face bending angle is more than 120° for the LAMIG joints. This is due to the improvement of weld formation and decrease of cross-section microhardness for the LAMIG welded joints.

In summary, LBW and LAMIG can be used to join medium strength Ti–Al–Zr–Fe titanium alloy. LBW may result in a rapid quench rate. With rapid cooling, those β grains convert to α′ as would be predicted by CCT diagram [12]. The fusion zone, which consists of α′ as the principal phase, would be of high cross-section microhardness and lack ductility. However, LAMIG can lead to a lower cooling rate, which may decrease the amounts of α′ in the fusion zone, and a broader fusion zone than LBW joint. LAMIG can also adjust the mechanical properties of welding seam by adding welding wires with different alloy elements. All in all, compared with LBW welded joints, it is obvious that the LAMIG welded joints have better combination of strength and ductility. The process of LAMIG welding is proved to be feasible for the production of titanium sheet joints.

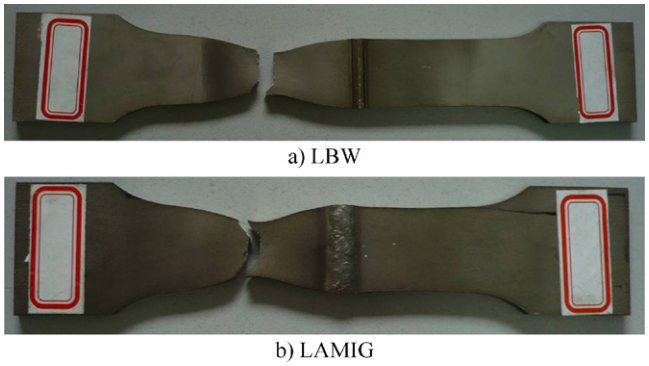

Fig. 6. A view of butt joints welded by LBW and LAMIG after tensile tests.

4. Conclusions

- 4 mm thick Ti–Al–Zr–Fe medium strength titanium alloy sheets were welded at a high speed of 1.8 m/min and power of 8 kW using LBW and LAMIG welding methods. All the welding joints obtained are of no defects, like oxidation, cracks, porosities and lack of penetration. LAMIG method can improve the weld formation by adding welding wire and higher heat input.
- LBW fusion zone consists of primary α′ as the principal phase at a rapid cooling rate. LAMIG method can adjust the microstructure of fusion zone with lower microhardness.
- All tensile specimens fractured at the parent metal, and face bending tests showed higher bending angles in the LAMIG welded joints.
- The LAMIG welded joints have better combination of strength and ductility. The process of the LAMIG welding is proved to be feasible for the production of titanium sheet joints.

References

[1] I. Gurrappa, Materials Characterization 51 (2–3) (2003) 131–139.
[2] Zhao Yongqing, Wei Jianfeng, Gao Zhanjun, et al., Materials Review 17 (4) (2003) 5–7 (in Chinese).
[3] Liu Yinqi, Meng Xiangjun, Liao Zhiqian, et al., Acta Metallurgica Sinica 38 (Suppl. 9) (2002) 264–266 (in Chinese).
[4] M. Balasubramanian, V. Jayabalan, V. Balasubramanian, Materials Letters 62 (6–7) (2008) 1102–1106.

[5] Qi Yunlian, Deng Ju, Hong Quan, Zeng, Liying, Materials Science and Engineering A 280 (2000) 177–181.
[6] V.I. Muravev, V.A. Kim, A.A. Shpileva, Metal Science and Heat Treatment 50 (3–4) (2008) 187–190.
[7] P. Wanjara, M. Brochu, M. Jahazi, Materials and Manufacturing Processes 21 (2006) 439–451.
[8] S.D. Meshram, T. Mohandas, Materials & Design 31 (4) (2010) 2245–2252.
[9] S. Prasad, Edward A.M. Jr., The Journal of Prosthetic Dentistry 101 (4) (2009) 221–225.
[10] M. Cabibbo, S. Marrone, E. Quadrini, Welding International 19 (2) (2005) 125–129.
[11] E. Akman, A. Demir, T. Canel, T. Sınmazçelik, Journal of Materials Processing Technology 209 (8) (2009) 3705–3713.
[12] J. Mazumder, W.M. Steen, Metallurgical Transactions 13A (1982) 1982–1985.
[13] Jun Yan, Ming Gao, Xiaoyan Zeng., Optics and Lasers in Engineering 48 (4) (2010) 512–517.
[14] Jun Yan, Xiaoyan Zeng, Ming Gao, Jian Lai, Tianxiao Lin., Applied Surface Science 255 (16) (2009) 7307–7313.
[15] P.E. Denny, B.W. Shinn, P. Mike Fallara, Proceedings of the 15th International Offshore and Polar Engineering Conference, Seoul, Korea, June 19–24, 2005, pp. 106–108.
[16] L. Cui, M. Kutusna, T. Simizu, K. Horio, Materials & Design 30 (1) (2009) 109–111.
[17] R. Fabbro, AIP Conference Proceeding, Laser and Plasma Applications in Materials Science 1047 (2008) 18–24.
[18] X. Cao, W. Wallacea, J.P. Immarigeona, C. Poon, Materials and Manufacturing Processes 18 (1) (2003) 23–49.